Axial radiation force of a Bessel beam on a sphere and direction reversal of the force

Philip L. Marston[a)]
Department of Physics and Astronomy, Washington State University, Pullman, Washington 99164-2814

(Received 1 September 2006; accepted 18 September 2006)

An expression is derived for the radiation force on a sphere placed on the axis of an ideal acoustic Bessel beam propagating in an inviscid fluid. The expression uses the partial-wave coefficients found in the analysis of the scattering when the sphere is placed in a plane wave traveling in the same external fluid. The Bessel beam is characterized by the cone angle β of its plane wave components where $\beta=0$ gives the limiting case of an ordinary plane wave. Examples are found for fluid spheres where the radiation force reverses in direction so the force is opposite the direction of the beam propagation. Negative axial forces are found to be correlated with conditions giving reduced backscattering by the beam. This condition may also be helpful in the design of acoustic tweezers for biophysical applications. Other potential applications include the manipulation of objects in microgravity. Islands in the (ka, β) parameter plane having a negative radiation force are calculated for the case of a hexane drop in water. Here k is the wave number and a is the drop radius. Low frequency approximations to the radiation force are noted for rigid, fluid, and elastic solid spheres in an inviscid fluid. © *2006 Acoustical Society of America.* [DOI: 10.1121/1.2361185]

PACS number(s): 43.25.Qp, 43.25.Uv, 43.20.Fn, 43.80.Jz [MFH] Pages: 3518–3524

I. INTRODUCTION

There have been numerous theoretical investigations of the acoustical radiation force of plane traveling waves (often referred to as progressive waves) incident on spherical objects in an inviscid fluid.[1–7] Some aspects of the radiation force of focused acoustic beams on spheres have also been calculated.[7–11] Some research suggests the possibility of trapping small objects (such as biological cells) near the focus of a single traveling wave.[10,11] The ability to either trap an object or pull it back toward the source of a single beam of sound may be a desirable alternative to the better known form of "acoustic tweezers" based on counterpropagating sound beams from a pair of transducers.[9] Such single-beam acoustic tweezers may provide an alternative to "optical tweezers" widely investigated for the purpose of trapping biological cells or other small objects.[12–15] In either the acoustic or electromagnetic case an important property of focused beams is that conditions have been predicted where the radiation force is in the opposite direction of the beam propagation even in the absence of significant dissipation. For *plane wave illumination* of spheres having isotropic properties in situations where dissipation can be neglected, the radiation force is directed along the direction of propagation for the reasons reviewed below in Sec. III.

The purpose of this paper is to calculate the radiation force caused by an acoustic Bessel beam[16–19] in an inviscid ideal fluid incident on a sphere having isotropic material properties in the case where the sphere is centered on the Bessel beam. As an example, the force is calculated for the case of a spherical drop of a hydrocarbon liquid in water. For an appropriate choice of frequency and Bessel beam parameters, the force is predicted to be opposite the direction of the beam propagation.

Scalar wave acoustic Bessel beams are an axisymmetric solution of the Helmholtz equation for the complex velocity potential of the form[20]

$$\psi_B(x,y,z) = \psi_0 \exp(i\kappa z) J_0(\mu \sqrt{(x^2+y^2)}), \tag{1}$$

where ψ_0 determines the beam amplitude, z and (x,y) denote the axial and transverse coordinates, κ and μ denote the axial and radial wave numbers, J_0 is a zero-order Bessel function, and $\kappa^2+\mu^2=k^2=(\omega/c_0)^2$, where c_0 denotes the phase velocity of the fluid. Here and in subsequent discussions of first order quantities the complex time factor of the form $\exp(-i\omega t)$ has been separated from the spatial dependence of complex functions. The complex first order acoustic velocity and pressure are $u_B=\nabla\psi_B$ and $p_B=i\omega\rho_0\psi_B$ where ρ_0 is the density of the surrounding fluid. The radiation force calculation uses Marston's solution[21] for the scattering of an ideal Bessel beam by a sphere centered on the beam. Relevant aspects of that solution are noted here in Appendix A.

An important parameter in the characterization of a Bessel beam is the cone angle β which describes the angle of the planar wave components of the beam relative to the z axis.[20–23] That angle is related to the parameters in Eq. (1) by

$$\beta = \arccos(\kappa/k) = \arcsin(\mu/k). \tag{2}$$

That angle is illustrated in Fig. 1 for the problem under consideration. The other important parameters in the evaluation of the radiation pressure are the wave-number-radius product ka of the sphere and the sphere's material properties relative to those of the surrounding fluid. As discussed in Sec. III, the usual plane wave limit[5,6] is recovered for the general radiation force expression Eq. (10) for the case $\beta=0$. As a con-

[a)]Electronic mail: marston@wsu.edu

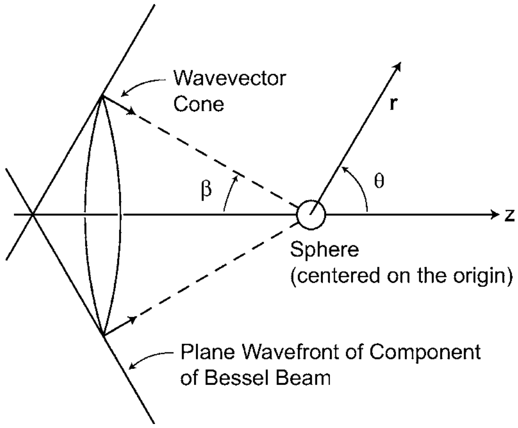

FIG. 1. Geometry of the radiation force calculation. The sphere is located on the axis z of an ideal Bessel beam. As explained in Refs. 20–22, the beam may represented by a superposition of plane waves having a cone angle β. The scattering angle relative to the beam axis is denoted by θ.

sequence of the finite width of all sources, Bessel-like beams only retain their form over a finite propagation distance.[16–23] The incident wave considered here is an ideal Bessel beam.

In addition to extending the understanding of situations where radiation forces are negative relative to the axis of a beam and related aspects of acoustic tweezers, some other potential applications of this analysis include the manipulation of fluid objects (such as liquid drops,[24,25] localized gas clouds,[26] or flames[27]) in reduced gravity (associated with space flight) where small forces acting over a long time duration can significantly affect the dynamics and positioning of objects. In addition since the analysis is sufficiently general to allow for the sphere to be metallic or ceramic there may be applications to the measurement of the acoustic intensity of approximate realizations of Bessel beams[16,18,22,23] as has long been the case for approximate realizations of plane waves.[3,4]

The present analysis completely ignores the complications resulting from thermal-viscous effects and from acoustic streaming. Analytical studies by Doinikov[28–30] indicate that there are numerous situations where such corrections to the radiation force may be especially significant for the case of traveling waves. For situations where the fluids used have sufficiently small viscosities, experiments have given satisfactory agreement with the inviscid radiation force of a traveling wave. Examples include low viscosity hydrocarbon liquid drops in water as well as the case of various solid spheres illuminated by quasiplane waves.[3,4] The thickness of the oscillating viscous external boundary layer (and in the liquid drop case, the thickness of oscillating internal boundary layer) must be much less than both the wavelength and the sphere radius a. It is assumed that this condition holds for the situation considered here. It is noteworthy that Doinikov[30] has predicted that as a consequence of *viscous corrections* a bubble may be attracted to a source of sound, however the mechanism in that case differs from the *inviscid radiation force* illustrated here for liquid drops.

II. RADIATION FORCE ON A SPHERE IN A BESSEL BEAM

It is convenient to evaluate the radiation force by using the farfield scattering summarized in Appendix A. The analysis of radiation forces based on farfield properties[27,31–33] is an alternative to the nearfield approach of King[1] and Yosioka and Kawasina.[2] The analysis is facilitated by the property of the radiation stress tensor[27,33] $\mathbf{S}_T$ for an ideal fluid that $\nabla \bullet \mathbf{S}_T = 0$. As a consequence, by application of the divergence theorem, the integral for the radiation force on the object can be transformed to a surface located at a large distance from the object.[27,33] In the present case this surface is taken to be a spherical surface of radius r with $kr \gg 1$. Let Re and Im designate real and imaginary parts of a complex quantity. The axial radiation force on the sphere is[33]

$$\mathsf{F}_z = -\pi \rho_0 k^2 (I_1 + I_2 - I_3), \tag{3}$$

$$I_1 = (\psi_0 a/2)^2 \int_{-1}^{1} |F(ka,w,b)|^2 w\,dw, \tag{4}$$

$$I_2 = (\psi_0 ra/2) \int_{-1}^{1} \mathrm{Re}[\psi_B^* F(ka,w,b) e^{ikr}] w\,dw, \tag{5}$$

$$I_3 = (\psi_0 ra/2k) \int_{-1}^{1} \mathrm{Im}[(\partial \psi_B/\partial z)^* F(ka,w,b) e^{ikr}] dw, \tag{6}$$

where $w = \cos\theta$, θ is the scattering angle shown in Fig. 1, $b = \cos\beta$, and * denotes complex conjugation. Equations (3)–(6) follow from Eq. (6) of Ref. 33 after expressing the scattering with the normalization used in Eq. (A1) in which the amplitude F is dimensionless. The expression has been simplified by taking the amplitude factor ψ_0 to be real and by omitting two terms proportional to ψ_0^2 (shown in Ref. 33) which do not contain F. The sum of the omitted terms vanishes. (The radiation force F_z vanishes when the scatterer is removed from the volume considered[27] so that then there is no scattering and $F=0$.) The integrals in Eqs. (4)–(6) may be evaluated in the limit of large kr by using the partial-wave representations of F and ψ_B given in Eqs. (A2), (A4), and (A6) and by using properties of the Legendre polynomials listed in Appendix B. The partial wave coefficients α_n and β_n are related by Eqs. (A3) and (A4) to the partial wave expansion of the scattering for plane wave incidence. The integrals reduce to

$$I_1 = (2\psi_0/k)^2 \sum_{n=0}^{\infty} (n+1)(\alpha_n \alpha_{n+1} + \beta_n \beta_{n+1}) P_n(b) P_{n+1}(b), \tag{7}$$

$$I_2 = (\psi_0/k)^2 \sum_{n=0}^{\infty} (n+1)(\alpha_n + \alpha_{n+1}) P_n(b) P_{n+1}(b), \tag{8}$$

$$I_3 = -(\kappa/k)(\psi_0/k)^2 \sum_{n=0}^{\infty} (2n+1) \alpha_n P_n^2(b). \tag{9}$$

Notice that $\kappa/k = \cos\beta = P_1(b)$. Using Eq. (B3), gives $I_3 = -I_2$. The acoustic intensity (in W/m^2) along the axis of the Bessel beam is $I_0 = (\rho_0 c_0/2)(\kappa k \psi_0^2) = (\rho_0 c_0/2)(k\psi_0)^2 \cos\beta$. The axial radiation force on the sphere becomes

$$\mathsf{F}_z = (\pi a^2)(I_0/c_0)(1/\cos\beta) Y_P(ka, \cos\beta), \tag{10a}$$

$$Y_P = -(2/ka)^2 \sum_{n=0}^{\infty} (n+1) \times [\alpha_n + \alpha_{n+1} + 2(\alpha_n \alpha_{n+1} + \beta_n \beta_{n+1})] \times P_n(\cos\beta) P_{n+1}(\cos\beta), \tag{10b}$$

where the normalization of the dimensionless function Y_P was selected for ease of comparison with standard results for plane traveling waves.[3–7] When β is 90° the product $P_n(\cos\beta)P_{n+1}(\cos\beta)$ vanishes for all n because either n or $n+1$ is odd. Consequently Y_P vanishes in that limit as required by symmetry.

III. RADIATION FORCE IN THE PLANE-WAVE LIMIT

In the limit of a plane traveling wave, $\cos\beta=1$ and $P_n(\cos\beta)=1$ for all n. Consequently Y_P reduces to the standard expression given by Hasegawa *et al.*[5,6] Notice that while the present derivation uses the $\exp(-i\omega t)$ convention and Hasagawa *et al.* use the $\exp(i\omega t)$ convention, the form of Y_P is retained since the dependence on β_n always appears as the product $\beta_n\beta_{n+1}$. This limit also agrees with a result for Y_P based on the $\exp(-i\omega t)$ convention.[34] For plane waves, Eqs. (8), (9), and (A2) give

$$I_2 - I_3 = -2I_3 = 2(\psi_0/k)^2 \sum_{n=0}^{\infty} (2n+1)\alpha_n = -ka(\psi_0/k)^2 \,\mathrm{Im}[f(ka,1)], \tag{11}$$

where $f(ka,\cos\theta)=F(ka,\cos\theta,1)$ is the dimensionless form function in the plane wave limit. In the case of a scatterer having no dissipation, $|s_n|=1$ and the optical theorem[35] gives for the imaginary part of the *forward scattering* form function,

$$\mathrm{Im}[f(ka,1)] = (ka/2)\int_0^{\pi} |f|^2 \sin\theta d\theta. \tag{12}$$

Combining Eqs. (3), (4), (10a), (11), and (12) gives in that case,

$$Y_P = (1/2)\int_0^{\pi} |f(ka,\cos\theta)|^2 (1-\cos\theta)\sin\theta d\theta, \tag{13}$$

which is *non-negative*. Equation (13) is equivalent to an early result of Westervelt[31] specialized to the case of no absorption and in the case of light scattering, an early result of Debye.[36,37] Inspection of Eq. (13) shows that the behavior of $|f|^2$ for θ near π is significantly weighted in the evaluation of Y_P. Reducing the scattering into the backward hemisphere reduces the radiation force. For a perfectly reflecting sphere having $ka \gg 1$, except near a narrow forward diffraction peak[21,35] $|f| \approx 1$ and Eq. (13) gives $Y_P \approx 1$. Including the absorption of a sphere introduces a positive term,[31] not in Eq. (13), which is proportional to the ratio of the absorption cross section to the geometric cross section πa^2.

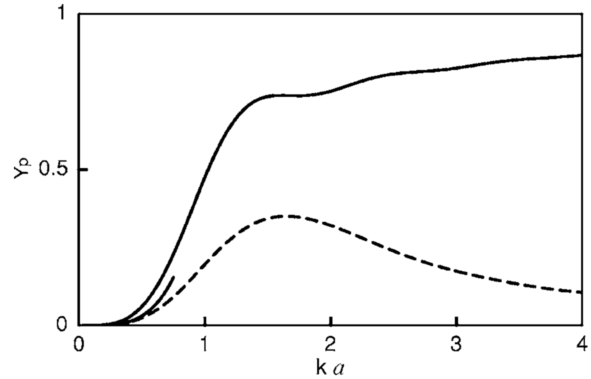

FIG. 2. Dimensionless radiation force function Y_P from Eq. (10b) for a fixed rigid sphere for an incident plane wave (upper solid curve) and an incident Bessel beam having $\beta=60°$. The results are expressed in terms of the size parameter ka for the sphere. The short lower solid curve is the low frequency approximation from Eq. (14) for $\beta=60°$.

IV. FORCE ON A RIGID SPHERE IN A BESSEL BEAM

Consider now the case of a fixed rigid sphere placed on the axis of a Bessel beam. In that case the s_n are given by[21] $s_n=-h_n^{(2)}(ka)'/h_n^{(1)}(ka)'$, where h_n is a spherical Hankel function of the indicated kind and primes denote differentiation. Figure 2 shows Y_P from Eq. (10b) for a plane wave (the upper solid curve) and a Bessel beam having $\beta=60°$ (the dashed curve). It was numerically found that the series in Eq. (10) may be truncated for n somewhat in excess of ka. A large value of β was selected so as to clearly show the reduction in Y_P. When ka is very small, less than approximately 0.3, the scattering is dominated by the monopole ($n=0$) and dipole ($n=1$) terms of Eq. (A2). Using Mathematica® to obtain the leading order term in the small ka expansion of Y_P, gives the following low frequency approximation:

$$Y_{\mathrm{PLF}}(ka,\cos\beta) = (ka)^4[1 + (2/9)P_2(\cos\beta)]P_1(\cos\beta). \tag{14}$$

Only s_0 and s_1 were found to influence Y_P to this order of ka. The lower solid curve in Fig. 2 shows Y_{PLF} when ka is small for $\beta=60°$. Comparison with the dashed curve shows that at small ka the result from Eq. (10b) is recovered. Taking $\beta=0$ in Eq. (14) gives $Y_P \approx (ka)^4(11/9)$, which is King's result[1] for a massive rigid sphere.

V. FORCE ON AN IDEAL FLUID SPHERE IN A BESSEL BEAM

In this case the s_n are given in Appendix A. When expressing the relative fluid properties it is convenient to use the dimensionless parameters of Yosioka and Kawasima[2] and of Lee and Wang[38] which are $\sigma=c_i/c_0$ and $\lambda=\rho_i/\rho_0$ for the inner-to-outer fluid sound speed and density ratios. In the plane wave case, the Y_P for several ka for a liquid drop having $\sigma=1/1.15$ and $\lambda=1.005$ were tabulated by Yosioka *et al.*[3] The numerical algorithm used here was found to agree with the tabulated values of Y_P. Crum[39] lists typical values of these ratios for immiscible hydrocarbon liquid drops *in water* at near room temperature conditions. The example of a liquid

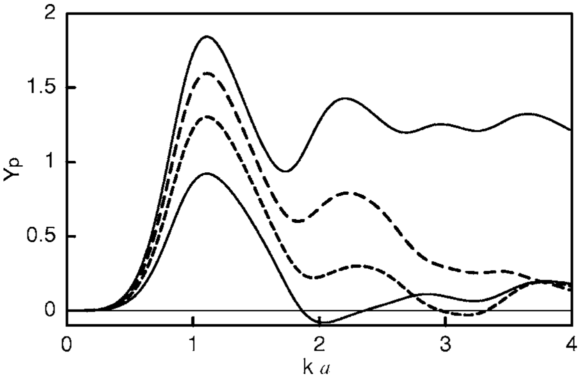

FIG. 3. Dimensionless radiation force function Y_P from Eq. (10b) for a sphere of ideal fluid having the relative properties of a liquid hexane drop in water for four values of β: 0° (upper solid curve), 30° (upper dashed curve), 45° (lower dashed curve), and 60° (lower solid curve). For β=45° and 60° there are regions where Y_P is negative so that the radiation force is directed opposite to the propagation direction of the Bessel beam.

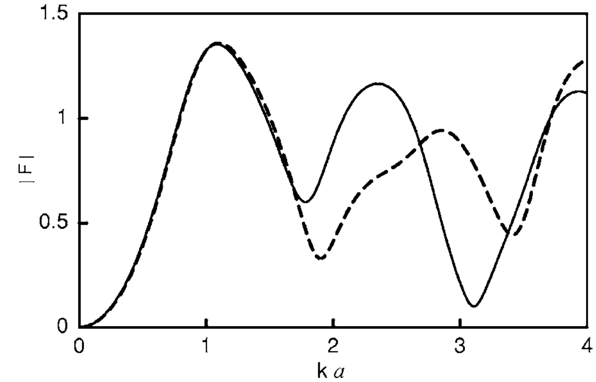

FIG. 4. Dimensionless form function magnitude from Eq. (A2) calculated for backscattering for the fluid sphere considered in Fig. 3 for β=45° (solid curve) and β=60° (dashed curve). The regions where Y_P is negative in Fig. 3 are associated with reduced backscattering.

drop in a Bessel beam considered in Fig. 3 is a hexane drop for which σ=0.719 and λ=0.656. Figure 3 shows Y_P for several values of β including the plane wave case. It was numerically found that the series in Eq. (10) may be truncated for n somewhat in excess of ka.

The anomalous regions where Y_P is negative are discussed in Sec. VI. Consider here the reduction in Y_P with increasing β when ka is less than 0.5. As reviewed in Sec. IV when ka is small the scattering is dominated by the monopole and dipole terms in Eq. (A2). Only those partial waves contribute to the leading order in the small ka expansion of Y_P. By using Mathematica® the leading order term in the low frequency approximation is found to be

$$Y_{\mathrm{PLF}} = [4(ka)^4/\Delta^2][G^2 + (2/9)(1-\lambda)^2 P_2(b)]\cos\beta, \tag{15a}$$

$$G(\lambda,\sigma) = \lambda - (\Delta/3\lambda\sigma^2), \tag{15b}$$

where $\Delta=1+2\lambda$ and $b=\cos\beta$. The result of Yosioka and Kawasima[2] (also found by Lee and Wang[38]) is recovered when β=0. Equation (15) shows that while the $\cos\beta$ factor causes a reduction in Y_{PLF} with increasing β, the dependence on β is complicated by the term involving $P_2(\cos\beta)$. The low-frequency approximation for an incompressible (but movable) sphere is found by taking the limit $\sigma^2\to\infty$ in Eq. (15b) so that G in Eq. (15a) is replaced by $G=\lambda$ where λ is the density ratio. In the plane wave limit Y_{PLF} reduces to $[4(ka)^4/\Delta^2][\lambda^2+(2/9)(1-\lambda)^2]$ in agreement with King's analysis for a movable incompressible sphere.[1] The fixed-rigid sphere limit for a Bessel beam, Eq. (14), is recovered by taking $\lambda\to\infty$ and $\sigma^2\to\infty$ in Eq. (15).

VI. NEGATIVE AXIAL RADIATION FORCES IN A BESSEL BEAM

Inspection of Fig. 3 reveals for β=45° and 60°, there are ka regions where Y_P becomes negative. When Y_P is negative the radiation force is directed opposite the direction of beam propagation. To understand the reversal in the direction of the force, recall from the plane-wave example discussed in Sec. III that the backscattering amplitude strongly influences Y_P. Figure 4 shows the backscattering form function magnitude $|F(ka,-1,\cos\beta)|$ for β=45° and 60° for the fluid sphere considered in Fig. 3. Inspection of Fig. 4 shows that there are prominent *minima* in $|F|$ for the regions where Y_P is negative. This property is also evident by comparing the θ dependence of $|F(ka,\cos\theta,\cos\beta)|$ for ka at or near the center of the regions where Y_P is negative with the case where β=0. Figure 5 shows this comparison for a hexane sphere with ka=3.17 in a beam with β=45°. The scattering in the entire backward hemisphere is suppressed in the Bessel beam case relative to the plane-wave case. Since ka is not large only a few partial waves contribute significantly to the scattering in Eq. (A2) and $|F|$ is found to be a slowly varying function of θ in comparison to large ka examples for rigid and soft spheres shown in Ref. 21. Inspection of Fig. 5 and Eq. (B2) suggests that scattering into the backward hemisphere is suppressed because the factor $P_n(\cos\beta)$ affects the significant partial waves. Figure 6 shows a similar comparison for β=60° and ka=2 which corresponds to a region where Y_P is negative. In that case, however, fewer partial waves are significant. The most negative value of Y_P for the example in Fig. 3 is Y_P=−0.081 at ka=2.03 for β=60°. For β=45° the most negative Y_P value is −0.0297 which is at

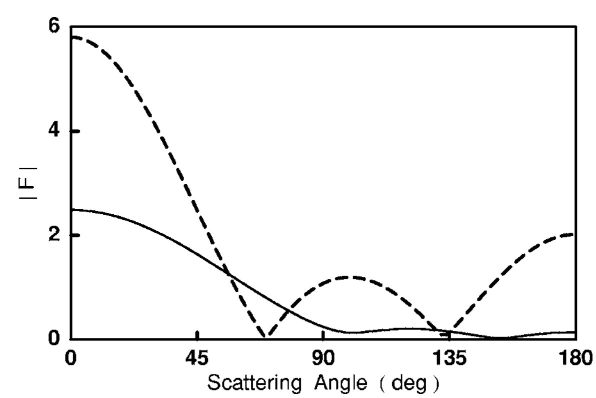

FIG. 5. The solid curve is the angular distribution of the scattering amplitude $|F|$ from Eq. (A2) for the liquid drop considered in Fig. 3 for a condition where Y_P is negative: ka=3.17 and β=45°. The dashed curve is for ka=3.17 with phase wave incidence (β=0°). The comparison shows that the scattering into the backward hemisphere is significantly depressed in the Bessel beam case.

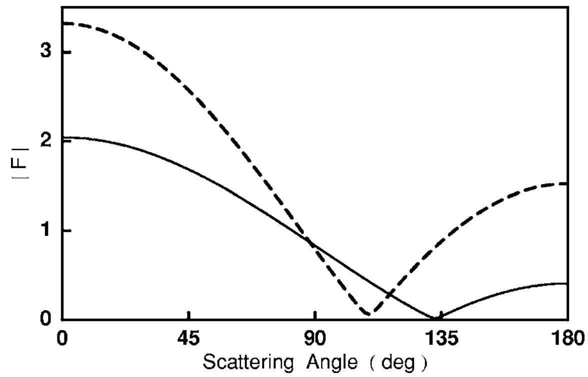

FIG. 6. Like Fig. 5 except that for the solid curve $ka=2$ and $\beta=60°$ and the dashed curve is $ka=2$ and $\beta=0°$.

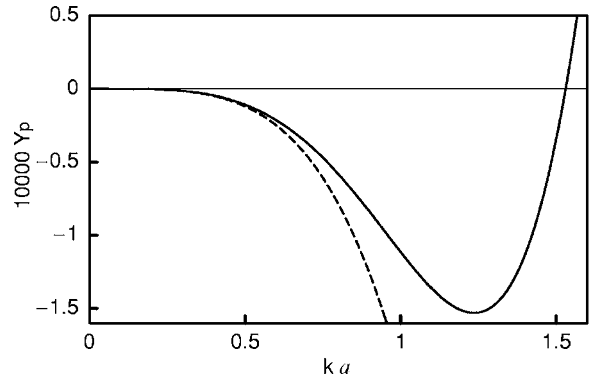

FIG. 8. The solid curve is Y_P from Eq. (10b) for a fluid sphere with relative fluid properties selected to give $G(\lambda,\sigma)=0$ in Eq. (15) by taking $\lambda=1.2$ and $\sigma=\sqrt{(3.4/4.32)}$. The dashed curve is the low frequency approximation in Eq. (15). The solid curve Y_P is negative for ka between 0 and 1.52.

$ka=3.17$. For $\beta=60°$ the small local *maximum* in Y_P in Fig. 3 at $ka=2.86$ corresponds to a local *maximum* in $|F|$ at $ka=2.85$ in Fig. 4.

To search for other regions having negative radiation force, Y_P from Eq. (10b) was evaluated for a sphere having the properties of an ideal hexane drop in water ($\sigma=0.719$, $\lambda=0.656$) for a dense grid of points on the region $0<ka<6$, $0°<\beta<90°$. Negative values were found only in the part with $1<ka<6$, $40°<\beta<90°$. Figure 7 shows that Y_P is negative on *islands* within that subregion. From symmetry and from the form of Eq. (10), Y_P vanishes when $\beta=90°$. For $\beta=30°$ with this σ and λ, Y_P was computed to be non-negative for $ka<20$.

A systematic search for regions of negative Y_P in the four parameter domain (ka, β, λ, σ) was beyond the scope of this investigation. Restricting attention to β of 45° and 60°, examples giving negative Y_P are easy to find even for spheres having different properties than hexane spheres in water. For a carbon tetrachloride sphere in water[39] ($\lambda=1.587$, $\sigma=0.619$) there are negative Y_P peaks at (ka, β, Y_P) of (2.98, 45°, −0.0269) and (2.29, 60°, −0.0309). For a benzene sphere in water[39] ($\lambda=0.874$, $\sigma=0.861$) there are negative Y_P peaks at (ka, β, Y_P) of (3.75, 45°, −0.00455) and (2.55, 60°, −0.0111).

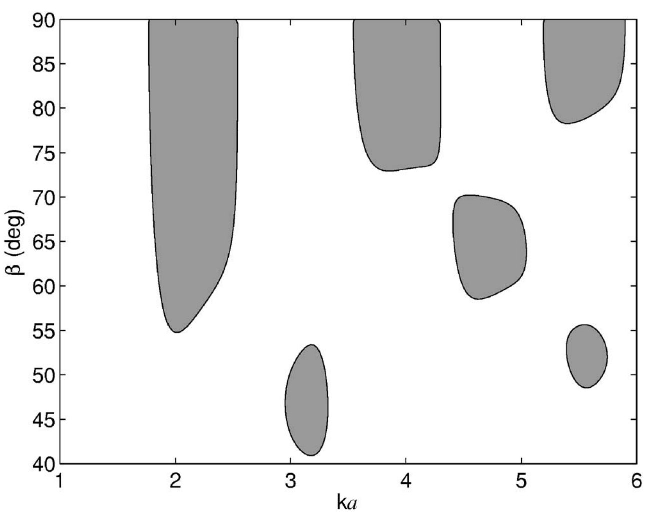

FIG. 7. Islands where Y_P is computed by Eq. (10b) to be negative are shown as dark patches that are bounded by a contour at $Y_P=0$. These are shown for a hexane sphere in water. The examples where Y_P is negative in Fig. 3 are in the leftmost islands.

Inspection of Eq. (15) suggests that for small ka, Y_P becomes negative when the fluid parameters λ and σ are selected to give $G(\lambda,\sigma)=0$. It is also necessary for β to lie between 54.7346° and 90° so that $P_2(\cos\beta)<0$ and $\cos\beta>0$. The condition $G(\lambda,\sigma)=0$ gives $\sigma=\sqrt{[(1+2\lambda)/(3\lambda^2)]}$. Figure 8 shows $10^4 Y_P$ for $\lambda=1.2$ and $\sigma=\sqrt{(3.4/4.32)}\approx 0.887$. Also shown is $10^4 Y_{\mathrm{PLF}}$ from Eq. (15). Notice that Y_P is negative as predicted but that when ka exceeds 1.52, Y_P becomes positive. As noted in Sec. V, Y_{PLF} is influenced by only the monopole and dipole scattering terms in Eq. (A2). Positive Y_P may be due to partial waves in Eq. (B2) with $n>1$. The 10^4 prefactor was included in Fig. 8 because of the very small magnitude of Y_P which is typically less than 10^{-4} in this region.

VII. DISCUSSION AND CONCLUSIONS

The main result in Eq. (10) gives the radiation force for an isotropic sphere centered on an ideal Bessel beam. The partial wave coefficients α_n and β_n are related by Eqs. (A3) and (A4) to the partial wave expansion of the scattering for plane wave incidence. The derivation of Eq. (10) was sufficiently general to allow for the case where the absorption of acoustic energy by the sphere cannot be neglected. This is often the case for plastic or polymer spheres placed in water.[5,40] Including absorption causes $|s_n|<1$ while the connection with α_n and β_n in Eq. (A4) remains applicable. In the numerical examples for Y_P and the analytical approximations of the low frequency behavior, Eqs. (14) and (15), absorption is neglected.

When absorption is negligible, the approximation in Eq. (15) becomes applicable to a small solid elastic sphere by taking the inner sound speed to be $c_i=\sqrt{[c_L^2-(4/3)c_T^2]}$ where c_L and c_T are the longitudinal and transverse wave velocities of the elastic material. That replacement has been shown to yield the proper monopole and dipole scattering contributions for the equivalent fluid sphere when ka is small in the present case where the viscous properties of the outer fluid are neglected.[41] For that replacement to be applicable it is necessary for ka to be much less than the ka of any low-frequency resonance, including that of the $n=2$ partial wave.[40]

The existence of conditions where Y_P becomes negative suggests that it may be feasible to point a Bessel beam at a sphere and use the acoustic radiation force to *pull the sphere back towards the source*. This application is plausible in reduced gravity (space-based platforms) where small radiation forces can significantly affect the motion of spheres over an extended period of time. For a more definitive analysis, however, it would be necessary to analyze the transverse force on the sphere for spheres displaced slightly from the axis of the Bessel beam. That analysis is outside the scope of the present discussion since Eqs. (10) and (A2) are only directly applicable for a sphere centered on a Bessel beam.

The comparison of Fig. 3 with plots of the scattering shown in Figs. 4–6 (and other results not shown here) indicate that the regions where Y_P is negative with a significant magnitude tend to occur where the backscattering amplitude is suppressed as a consequence of the illumination by a Bessel beam. It is plausible that this correlation with backscattering may be used to find regions of enhanced performance of acoustic tweezers or other devices for biophysical applications.[9–11,42] When ka is small so that Eq. (15) is applicable, from the example in Fig. 8, negative Y_P appear unfortunately to be small in magnitude.

Concerning the unresolved question of the transverse stability of spheres on the axis of a Bessel beam, the following observations are noteworthy. Liquid filled circular cylindrical acoustic levitators produce a standing wave pressure distribution where the radial dependence of the pressure is typically of the form $J_0(\mu\sqrt{(x^2+y^2)})$ as in the Bessel beam case. Numerous examples have been demonstrated where small drops and bubbles in water (or in other liquids) are attracted to the axis of such cylinders.[24,39,43,44] Much less is known about the radial stability when ka is not small. The mathematical existence of conditions for ideal spheres to have transverse stability in acoustic Gaussian beams[11] makes it plausible that conditions can also be found for acoustic Bessel beams. The existence of transverse stability of objects trapped in light beams is also supportive.[12–15] Ordinarily transverse stability of gas bubbles in liquids subjected to the *optical* radiation pressure of a laser beam requires that the beam has an axial irradiance minimum.[45] Stability of bubbles in light beams of a different type was recently demonstrated.[46] If necessary the transverse stability of spheres in *acoustic* Bessel beams could be altered by superposing a second acoustic beam (at a different frequency) having an axial pressure minimum.[47]

ACKNOWLEDGMENTS

This research was supported in part by NASA. Appendix A and Ref. 21 were supported by ONR. The author is grateful to Dr. David B. Thiessen for helpful comments.

APPENDIX A: FARFIELD SCATTERING BY A SPHERE

For a sphere having isotropic material properties centered on the Bessel beam and placed at $z=0$, using the coordinate system shown in Fig. 1, the farfield scattering is given by

$$\psi_s(r,\theta) = (a/2r)\psi_0 F e^{ikr}, \tag{A1}$$

where the partial wave series for the dimensionless form function is found to be[21]

$$F(ka,\cos\theta,\cos\beta) = (-i/ka)\sum_{n=0}^{\infty}(2n+1)(s_n-1) \times P_n(\cos\theta)P_n(\cos\beta). \tag{A2}$$

The scattering angle relative to the z axis is denoted by θ. Here the coefficient (s_n-1) is the same as the partial wave coefficient for the dimensionless form function associated with scattering caused by plane wave illumination[35]

$$f(ka,\cos\theta) = (-i/ka)\sum_{n=0}^{\infty}(2n+1)(s_n-1)P_n(\cos\theta). \tag{A3}$$

It is convenient for the purposes of the present paper to introduce a normalized partial wave coefficient $\alpha_n+i\beta_n=(s_n-1)/2$ where

$$\alpha_n = [\mathrm{Re}(s_n)-1]/2, \quad \beta_n = \mathrm{Im}(s_n)/2 \tag{A4}$$

and Re and Im designate real and imaginary parts. As reviewed in Ref. 21, the s_n and the factors (s_n-1) are known for many types of spheres. When none of the incident acoustic energy is absorbed, the complex s_n are unimodular.[35] For example in the case of an inviscid fluid sphere s_n is given by $s_n=-D_n^*/D_n$ where the denominator is[48]

$$D_n = \rho_i ka j_n(ka/\sigma)h_n^{(1)\prime}(ka) - \rho_0(ka/\sigma)j_n'(ka/\sigma)h_n^{(1)}(ka), \tag{A5}$$

ρ_i and ρ_0 are the densities of the sphere and the surrounding fluid and $\sigma=c_i/c_0$ is the corresponding ratio of sound velocities. In Eq. (A5), primes denote differentiation of spherical Bessel and Hankel functions and * denotes complex conjugation.

The partial wave series for the incident wave, the Bessel beam in Eq. (1), is[21]

$$\psi_B = \psi_0\sum_{n=0}^{\infty} i^n(2n+1)j_n(kr)P_n(\cos\theta)P_n(\cos\beta). \tag{A6}$$

APPENDIX B: PROPERTIES OF LEGENDRE POLYNOMIALS

Properties of the $P_n(w)$ used in the derivation of Eqs. (7)–(10) include[49]

$$\int_{-1}^{1} P_m(w)P_n(w)dw = [2/(2n+1)]\delta_{mn}, \tag{B1}$$

$$\int_{-1}^{1} wP_m(w)P_n(w)dw = I_{mn}, \tag{B2}$$

where $I_{mn}=0$ unless $m=n\pm1$, $I_{n+1n}=2(n+1)/[(2n+1)(2n+3)]$ and $I_{n-1n}=2n/[(2n-1)(2n+1)]$. The following[49] was also used:

$$(n+1)P_{n+1}(w) - (2n+1)wP_n(w) + nP_{n-1}(w) = 0. \tag{B3}$$

The following special cases are noteworthy: $P_0(w)=1$, $P_1(w)=w$, $P_2(w)=(3w^2-1)/2$, and $P_2(\cos\beta)=0$ for $\beta=54.7356°$.

[1] L. V. King, "On the acoustic radiation pressure on spheres," Proc. R. Soc. London **147**, 212–240 (1934).

[2] K. Yosioka and Y. Kawasima, "Acoustic radiation pressure on a compressible sphere," Acustica **5**, 167–173 (1955).

[3] K. Yosioka, T. Hasegawa, and A. Omura, "Comparison of ultrasonic intensity from radiation force on steel spheres with that on liquid spheres," Acustica **22**, 145–152 (1969).

[4] T. Hasegawa and K. Yosioka, "Acoustic radiation force on fused silica spheres, and intensity determination," J. Acoust. Soc. Am. **58**, 581–585 (1975).

[5] T. Hasegawa and Y. Watanabe, "Acoustic radiation pressure on an absorbing sphere," J. Acoust. Soc. Am. **63**, 1733–1737 (1978).

[6] T. Hasegawa, Y. Hino, A. Annou, H. Noda, M. Kato, and N. Inoue, "Acoustic radiation pressure acting on spherical and cylindrical shells," J. Acoust. Soc. Am. **93**, 154–161 (1993).

[7] X. C. Chen and R. E. Apfel, "Radiation force on a spherical object in an axisymmetric wave field and its application to the calibration of high-frequency transducers," J. Acoust. Soc. Am. **99**, 713–724 (1996).

[8] J. R. Wu and G. Du, "Acoustic radiation force on a small compressible sphere in a focused beam," J. Acoust. Soc. Am. **87**, 997–1003 (1990).

[9] J. R. Wu, "Acoustical tweezers," J. Acoust. Soc. Am. **89**, 2140–2143 (1991).

[10] J. W. Lee, K. L. Ha, and K. K. Shung, "A theoretical study of the feasibility of acoustical tweezers: Ray acoustics approach," J. Acoust. Soc. Am. **117**, 3273–3280 (2005).

[11] J. W. Lee and K. K. Shung, "Radiation forces exerted on arbitrarily located sphere by acoustic tweezer," J. Acoust. Soc. Am. **120**, 1084–1094 (2006).

[12] A. Ashkin, J. M. Dziedzic, J. E. Bjorkholm, and S. Chu, "Observation of a single-beam gradient force optical trap for dielectric particles," Opt. Lett. **11**, 288–290 (1986).

[13] A. Ashkin, "Forces of a single beam gradient laser trap on a dielectric sphere in the ray optics regime," Biophys. J. **61**, 569–582 (1992).

[14] K. Svoboda and S. M. Block, "Biological applications of optical forces," Annu. Rev. Biophys. Biomol. Struct. **23**, 247–285 (1994).

[15] J. A. Lock, S. Y. Wrbanek, and K. E. Weiland, "Scattering of a tightly focused beam by an optically trapped particle," Appl. Opt. **45**, 3634–3645 (2006).

[16] D. K. Hsu, F. J. Margetan, and D. O. Thompson, "Bessel beam ultrasonic transducer: Fabrication method and experimental results," Appl. Phys. Lett. **55**, 2066–2068 (1989).

[17] J. A. Campbell and S. Soloway, "Generation of a nondiffracting beam with frequency-independent beamwidth," J. Acoust. Soc. Am. **88**, 2467–2477 (1990).

[18] J.-y. Lu and J. F. Greenleaf, "Ultrasonic nondiffracting transducer for medical ultrasonics," IEEE Trans. Ultrason. Ferroelectr. Freq. Control **37**, 438–447 (1990).

[19] K. B. Cunningham and M. F. Hamilton, "Bessel beams of finite amplitude in absorbing fluids," J. Acoust. Soc. Am. **108**, 519–525 (2000).

[20] J. Durnin, "Exact solutions for nondiffracting beams. I. The scalar theory," J. Opt. Soc. Am. A **4**, 651–654 (1987).

[21] P. L. Marston, "Scattering of a Bessel beam by a sphere," (submitted).

[22] J. Durnin, J. J. Miceli, Jr., and J. H. Eberly, "Diffraction-free beams," Phys. Rev. Lett. **58**, 1499–1501 (1987).

[23] D. McGloin and K. Dholakia, "Bessel beams: Diffraction in a new light," Contemp. Phys. **46**, 15–28 (2005).

[24] P. L. Marston and D. B. Thiessen, "Manipulation of fluid objects with acoustic radiation pressure," Ann. N.Y. Acad. Sci. **1027**, 414–434 (2004).

[25] S. K. Chung and E. H. Trinh, "Containerless protein crystal growth in rotating levitated drops," J. Cryst. Growth **194**, 384–397 (1998).

[26] R. Tuckermann, B. Neidhart, E. G. Lierke, and S. Bauerecker, "Trapping of heavy gases in stationary ultrasonic fields," Chem. Phys. Lett. **363**, 349–354 (2002).

[27] W. Wei, D. B. Thiessen, and P. L. Marston, "Acoustic radiation force on a compressible cylinder in a standing wave," J. Acoust. Soc. Am. **116**, 201–208 (2004).

[28] A. A. Doinikov, "Acoustic radiation pressure on a rigid sphere in a viscous fluid," Proc. R. Soc. London, Ser. A **447**, 447–466 (1994).

[29] A. A. Doinikov, "Acoustic radiation force on a spherical particle in a viscous heat-conducting fluid. III. Force on a liquid drop," J. Acoust. Soc. Am. **101**, 731–740 (1997).

[30] A. A. Doinikov, "Acoustic radiation pressure exerted by a spherical wave on a bubble in a viscous liquid," Wave Motion **24**, 275–279 (1996).

[31] P. J. Westervelt, "The theory of steady forces caused by sound waves," J. Acoust. Soc. Am. **23**, 312–315 (1951).

[32] L. P. Gorkov, "On the forces acting on a small particle in an acoustical field in an ideal fluid," Sov. Phys. Dokl. **6**, 773–775 (1962).

[33] C. P. Lee and T. G. Wang, "Acoustic radiation force on a bubble," J. Acoust. Soc. Am. **93**, 1637–1640 (1993).

[34] F. G. Mitri, "Acoustic radiation force due to incident plane-progressive waves on coated spheres immersed in ideal fluids," Eur. Phys. J. B **43**, 379–386 (2005).

[35] P. L. Marston, "Generalized optical theorem for scatterers having inversion symmetry: Applications to acoustic backscattering," J. Acoust. Soc. Am. **109**, 1291–1295 (2001).

[36] P. Debye, "Der Lichtdruck auf Kugeln von beliebigem Material," Ann. Phys. **30**, 57–136 (1909).

[37] H. C. van de Hulst, *Light Scattering by Small Particles* (Wiley, New York, 1957), pp. 124–130.

[38] C. P. Lee and T. G. Wang, "Radiation pressure and acoustic levitation," *Nonlinear Acoustics*, edited by M. F. Hamilton and D. T. Blackstock (Academic, New York, 1998), pp. 177–205.

[39] L. A. Crum, "Acoustic force on a liquid droplet in an acoustic stationary wave," J. Acoust. Soc. Am. **50**, 157–163 (1971).

[40] B. T. Hefner and P. L. Marston, "Backscattering enhancements associated with subsonic Rayleigh waves on polymer spheres in water: Observation and modeling for acrylic spheres," J. Acoust. Soc. Am. **107**, 1930–1936 (2000).

[41] R. A. Roy and R. E. Apfel, "Mechanical characterization of microparticles by scattered ultrasound," J. Acoust. Soc. Am. **87**, 2332–2341 (1990).

[42] W. T. Coakley, "Ultrasonic separations in analytical biotechnology," Trends Biotechnol. **15**, 506–511 (1997).

[43] R. E. Apfel, "Technique for measuring the adiabatic compressibility, density, and sound speed of submicroliter liquid samples," J. Acoust. Soc. Am. **59**, 339–343 (1976).

[44] D. F. Gaitan, L. A. Crum, C. C. Church, and R. A. Roy, "Sonoluninescence and bubble dynamics for a single, stable, cavitation bubble," J. Acoust. Soc. Am. **91**, 3166–3183 (1992).

[45] B. T. Unger and P. L. Marston, "Optical levitation of bubbles in water by the radiation pressure of a laser beam: An acoustically quiet levitator," J. Acoust. Soc. Am. **83**, 970–975 (1988).

[46] J. Y. Ye, G. Chang, T. B. Norris, C. Tse, M. J. Zohdy, K. W. Hollman, M. O'Donnell, and J. R. Baker, Jr., "Trapping cavitation bubbles with a self-focused laser beam," Opt. Lett. **29**, 2136–2138 (2004).

[47] B. T. Hefner and P. L. Marston, "An acoustical helicoidal wave transducer with applications for the alignment of ultrasonic and underwater systems," J. Acoust. Soc. Am. **106**, 3313–3316 (1999).

[48] K. A. Sage, J. George, and H. Uberall, "Multipole resonances in sound scattering from gas bubbles in a liquid," J. Acoust. Soc. Am. **65**, 1413–1422 (1979).

[49] J. D. Jackson, *Classical Electrodynamics*, 3rd ed. (Wiley, New York, 1999), Sec. 3.2, pp. 96–101.